Performance of a Brackish Water Desalination Unit Coupled to a Photovoltaic Source without Energy Storage

Boussaibo André[1], Kamta Martin[2], Badohok Sarki[3], Kayem Joseph[4]

[1]Department of Electrical Engineering, IUT, University of Ngaoundere
Ngaoundere, Cameroon, E-mail: *boussaibo@yahoo.fr**

[2] Department of Electrical, Energetic and Automatic Engineering, ENSAI, University of Ngaoundere
Ngaoundere, Cameroon, E-mail: *martin_kamta@yahoo.fr*

[3]Chemical and Environment Laboratory, IUT, University of Ngaoundere
Ngaoundere, Cameroon, E-mail: *sarki.badohock@yahoo.fr*

[4]Department of Process Engineering, ENSAI,University of Ngaoundere
Ngaoundere, Cameroon, E-mail: *gjkayem@yahoo.fr*

Abstract: The paper relates mainly on the characterization of brackish water desalination unit coupled to photovoltaic source. It aims to contribute to the improvement of the living conditions of the populations in remote rural areas, who have difficulties in accessing to drinking water and to the grid connected power supply. To evaluate the performance of the actual desalination unit, its operating parameters such as: frequency of motor pump, feed water pressure and corresponding flow rate of permeate are adjusted using the synthetic water solutions of sodium chloride, sodium sulfate and sodium bicarbonate respectively. So, the membrane retention rate as well as the conversion rate of the desalination unit could be evaluated. This desalination unit has been used for filtering brackish water from two wells and on borehole in Figuil city of Cameroon. The physicochemical analyses of the resulting permeate showed a good accordance with the WHO standards.

Keywords: Brackish Water, Desalination, Photovoltaic

I. INTRODUCTION

Water scarcity is a growing problem in many areas of the world, with increasing pressure from population growth [1]. Worldwide populations suffer of water scarcity in many arid and desert areas [2]. Therefore, it is necessary to resort to underground resources. However, most of the aquifers have been over-exploited and also suffer serious problems of saline contamination [3]. The contamination can be physical, chemical and bacteriological [4]. During the filtration process in soil, water load of dissolved mineral salts, which can be harmful (presence of excess nitrate or fluoride), unpleasant for consumption (excess iron and manganese) or brackish. Tests on samples of well water in different parts in Ngaoundere/Cameroon are conducted [5]. The analytical results show that, the water from these wells encountered for some, greater amounts of total dissolved solids than the WHO standard. In the floodplain of the Logone in the Far North of Cameroon, the lowest amount of total dissolved solids estimated to 279 mg/l is measured in the northeast of Bongor and between Katoa and Logone Gana on both sides of the Logone river [6]. The highest amounts average of 598 mg/l are obtained in the area adjacent to the Mandara mountains, in the south and north-west of Maga lake in Cameroon [6].

Following these observations, the desalination of brackish water appears as one of the main options to overcome water scarcity in arid and desert areas, particular in remote rural areas. Around 80% of brackish water desalination systems in the world use reverse osmosis (RO) [7]. But the almost total absence of conventional power source in remote rural areas is an obstacle to supply reverse osmosis system. The coupling of desalination unit to photovoltaic panel is therefore a suitable solution in these areas where the potential of solar radiation is significant and estimated to 7 kWh/m²/day in sahelian zones [8]. However, reverse osmosis systems require water at constant pressure and constant flow. Because of its fluctuation, photovoltaic power supply is not suitable to be directly coupled to reverse osmosis unit. To overcome these difficulties, a blocking algorithm of the duty ratio of the control signal of a hydraulic pump powered by a photovoltaic panel without batteries, was used to maintain a constant flow rate and pressure of water [9].
To achieve the purpose reached by this paper, electromechanical operating parameters of hydraulic pump are evaluated. Otherwise, the performance of a desalination unit by filtration tests on synthetic and natural water taken from wells in the city of Figuil/Cameroon is estimated.

II. MATERIAL AND METHOD

A. Experimental material

The diagram in fig.1 describes the desalination unit used. The PV panels, DC / DC converter, DC / AC converter and MPPT blocks are more detailed in preliminary work to this paper [9]. The tank to which the water intake is connected is placed one meter in height from the feed pump. This configuration was chosen to avoid the vacuum pump startup causing the suction of air in the pipes. The filtration unit is the EC105P model. It essentially consists of a pressure pump and five filter cartridges. The first cartridge is a 5-micron sediment filter whose role is to remove dust, particles and rusts. The second cartridge is a carbon filter. The third cartridge is a 1 micron sediment filter. It removes dust, particles and rusts. The fourth cartridge is a TFC membrane (Thin Film Composite) so the model is TW30-1812-50 TFC capable of producing an average of 189 liters/day. The fifth cartridge is a carbon filter. It removes residual impurities, odors and improves the taste. The working pressure of the filtration unit is between 5 and 80 psi. Various measuring devices are connected to allow the measurement of mechanical, hydraulic and pneumatic parameters.

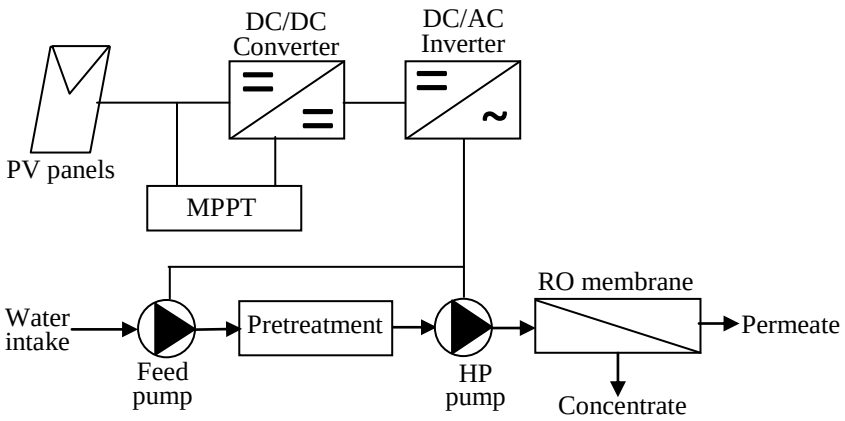

Figure 1: Experimental equipment

B. Sizing de photovoltaic power

The energy required for desalination resulted from the supplying of reverse osmosis unit and the supplying of feed pumping system. For this project, the desalination plant is designed to be located near the well. The power for desalination is expressed as following in (1):

$$P_{desal} = P_{OI} + P_{pump} \quad (1)$$

$$P_{desal} = \left(\frac{Q \times \gamma \times WD}{\eta}\right) + (Q \times 0.08 \times (TDS_{in} - TDS_{out})) \quad [10] \quad (2)$$

Where:

P_{desal}= useful power desalination (W),
γ= specific weight of water (N/m^3),
WD= well depth (m),
η = pump efficiency,
TDS_{in}= total dissolved solid in feed water (mg/l),
TDS_{out}= total dissolved solid in permeate (mg/l),
Q= volumetric flow rate of water (m^3/s).

As the desalination system is supplied by PV source, (3) and (4) below are used for calculating respectively the power of the PV system needed and the average daily energy:

$$P_{PV} = \eta_{PV} \times \eta_b \times F_{PV} \times Q_s \quad [11] \quad (3)$$

$$E = \eta_{PV} \times \eta_b \times F_{PV} \times Q_s \times \tau \quad (4)$$

Where:

P_{PV}= power of the PV system (W),
η_{PV}= PV generator efficiency,
η_b= batteries efficiency,
F_{PV}= surface of the PV field to install (m^2),
Q_s = average daily solar irradiation ($Wh/m^2/day$),
τ= average sunny hours.

In the absence of batteries, as is the context of this work, (5) is used to determine the surface PV field to be installed.

$$Q = \frac{\eta_{PV} \times F_{PV} \times Q_s \times \tau}{\left(\frac{\gamma \times WD}{\eta}\right) + (0.08 \times (TDS_{in} - TDS_{out}))} \quad [12] \quad (5)$$

Otherwise,

$$F_{PV} = \frac{Q\left[\left(\frac{\gamma \times WD}{\eta}\right) + (0.08 \times (TDS_{in} - TDS_{out}))\right]}{\eta_{PV} \times Q_s \times \tau} \quad (6)$$

Specially for this work, TDS_{in}, TDS_{out}, and the volumetric flow rate are obtained from tests on desalination pilot. The specific weight of water is taken from literature. The average sunny hour and the daily solar irradiation are those corresponding to the study area.

C. Preparation of synthetics solution

For a given solution, 100 liters of demineralised water previously produced is loaded into the tank. The measured conductivity of the demineralised water has an average value less than 3 µS/cm. For each salt, a solution is prepared according to the characteristic shown in the table 1 below.

Table 1: Feeds solution characteristics

Salts	Conductivity ($\mu S/cm$)	Molar concentration (mol/l)	Mass concentration (g/l)
Sodium chloride	5.7	5.128×10^{-2}	3
Sodium sulfate	5.1	2.82×10^{-2}	4
sodium bicarbonate	5.3	7.14×10^{-2}	6

After loading demineralised water in the tank, the next step is to prepare a stock solution in a beaker. The salt is progressively introduced into the beaker under continuous stirring. The stock solution is introduced into the feed tank under stirring for 3 hours. The pH of the solution in the feed tank is adjusted to 7 by the introduction of a solution of sodium hydroxide at 10^{-2} mol/l, to approach the pH of drinking water that ranges from 6.5 to 8.5 [13].

D. Sampling sites of natural water

Figuil is at 9°45' of North latitude and at 13°57' of East longitude, at an average altitude of 295 m. The chemical analysis of water in Figuil city reveals that groundwater is charged with carbon dioxide over 250 mg/l [14]. Moreover, in the rainy season, these layers undergo the "nitrification" due to the use of nitrate mixed with sygmagel and nitram 09 (70/200) in the explosives used to slaughter rocks by mining corporations installed in the area. Three water points designated "Borehole C" (Cimencam borehole), "Well R" (Rocaglia well) and "Well L" (Lamorde well) were selected in three different neighborhoods. The GPS coordinates of the sampling points are presented in Table 2.

Table 2: Sampling points

Parameters	Borehole C	Well R	Well L
Sampling date/time	24-04-2016/8h05	24-04-2016/9h21	24-04-2016/10h41
Depth (m)	30	9.5	5
Latitude	9°46'29" N	9°45'37" N	9°45'20"N
Longitude	13°57'52" E	13°57'54" E	13°57'55"E

Three criteria guided the choice of sampling points. The first is the availability of water during the period of sampling. The field visit was made in April, period during which some wells dry up in the area of Figuil. The second is on different depth of sampling points as shown in table 2. The third is the using conditions of sampling points. The combination of the three selection criteria have guided us to choose:

- "Borehole C". This sampling point is the deepest than the others and estimated to 30 m. The tank collecting water right out of the borehole is covered and protected from any physicochemical exchange with the ambient environment.
- "Well R". The depth of this sampling point is estimated to 9.5 m. The well is surmounted by curbstone of approximately 0.8 m height but not protected by a lid. It is therefore exposed to all kinds of contamination by exchanges with the environment, either by air or by the scoop which is deposited on the ground.
- "Well L" is the shallowest of the three sampling points. The well is surmounted by curbstone of approximately 0.5 m height and protected by a sheet aluminum lid. The protection against external contamination is not guaranteed because of negligence in the closure of the well after each use, and due to negligence occasionally in keeping the scoop on the ground.

E. Procedures for sampling

For each sampling point selected, three samples were collected. Samples of water to be analyzed was carried out in bottles of polyethylene of 0.5 liters, emptied from their contained on site and rinsed several times to avoid any contamination. The bottles are filled up overflow to prevent the penetration of air bubbles. They are then corked and labelled on origin of water, date and time of collection. Water samples for TA-TAC analyzes, chloride ions, phosphate ions, nitrate ions, nitrite ions, sulfate ions and ammonia nitrogen are conditioned without any chemical compound. The pH of water samples for COD and organic carbon analysis is corrected to be less than 2 using sulfuric acid. The pH of water samples for hardness tests is corrected to be less than 2 using nitric acid. Analyzes of parameters easily influenced by the variation of temperature and by the conservation summers have made in-situ. They are parameters such as conductivity, temperature, pH, TDS, dissolved oxygen and turbidity. Transport of samples from the sampling point to laboratory was made in a cooler at 4°C. When samples are stored, they are put in the refrigerator.

III. RESULTS

A. Operating conditions

Electromechanical characterization of hydraulic pump

Different tests were carried out to determinate electrical and mechanical characterization of the desalination unit. The electrical power absorbed and the rotation speed are measured at different operating frequencies of the induction motor.

The pump not start at the frequencies below 16 Hz. The profiles of power and speed curves are linear functions of the motor operating frequency as shown in fig.2 following. In order for the system to pump water, the minimum rotational speed and the corresponding power consumption are respectively estimated to 860 rpm and 276 W.

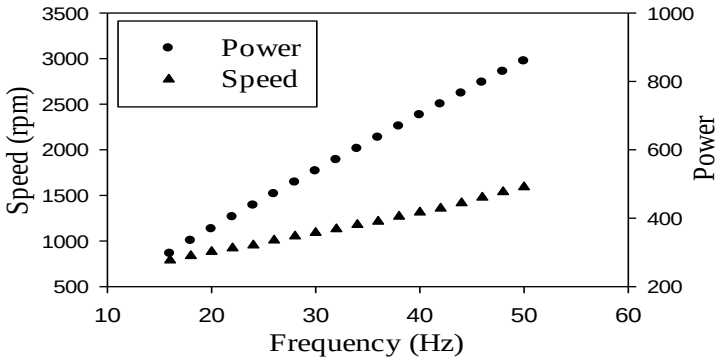

Figure 2: Variation in the power and speed depending on the operating frequency of motor

Hydraulic characterization of pilot unit

Different tests were also carried out for the hydraulic characterization of the pilot unit. Fig.3 shows the flow rate profiles of feed water and outlet water of desalination unit at different operating frequencies. Outlet water means the total of permeate and concentrate.

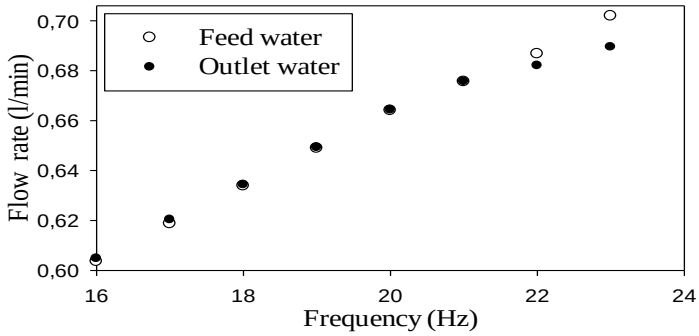

Figure 3: Variation of the feed flow rate and outlet flow rate depending on the operating frequency of motor.

The profiles of curves can be subdivided into three operating areas. A first area is bounded by ranging of frequencies from 16 to 18 Hz. In this area, the two curves are slightly displaced from each other from the frequency 16 Hz and converge at the frequency 18 Hz. The second area covers the frequencies from 18 to 21 Hz. Especially in this area, the curves overlap point by point. The third area is bounded by frequencies above 21Hz. The two curves diverge from the frequency 21 Hz to the end of the measuring ranges.

After analysis, specific phenomenon due to the slightly displaced of the curves is identified in the first area. This phenomenon shows that the flow rate of osmosis pump is greater than the flow rate of feed pump. It can be deducing that the outflow of reverse osmosis pump is slightly higher than the inflow. This phenomenon which may be at the origin of the cavitation of the pump [15]. In another case, the underfeeding of reverse osmosis pump will causes its heating. This warming will increases the temperature of water and modified consequently its viscosity. This will have negative impact on the conversion rate and the retention rate of the membrane [16]. Following these various disadvantages, we can conclude in this regard that the first operating area must be classified forbidden. Regarding the second area, it is apparent from the analysis of curves that the flow rate of osmosis pump is equal to the flow rate of feed pump. Consequently, the system operates under a balanced and stable regime. This area is also the common linear region to the both curves. For the third areas, the flow rate of feed pump is greater than the flow rate of osmosis pump. When the system is maintained on function in these frequencies, it is exposed to the piping explosion risk because of the overpressure caused by the imbalance between the inflow and outflow [15]. The overpressure corresponding to pressure exceed 1.8 bar according to the curve of fig.4. It can be concluded in this regard that the third operation area must also be classified as prohibited area.

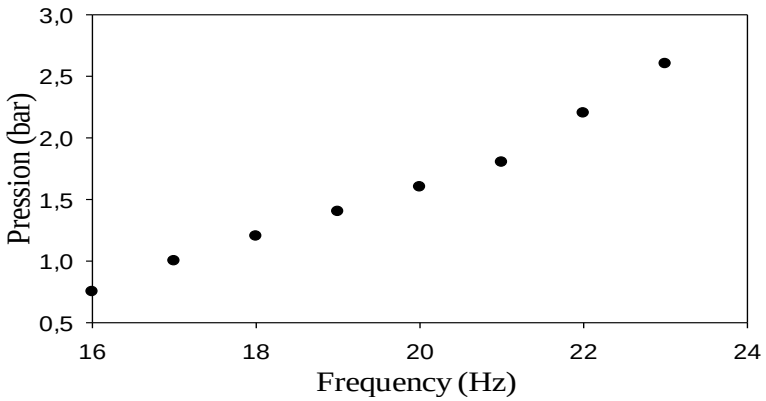

Figure 4: Variation of the feed pressure depending on the operating frequency of motor.

The analysis of the three operating areas allows to conclude that the second is the safety area of the desalination pilot. For the rest of the work, experiments are carried out at the operating frequency of 21 Hz. It is the frequency in the area of safety allowing to product the greatest flow rate of permeate estimated to 0.116 l/min according to fig.5.

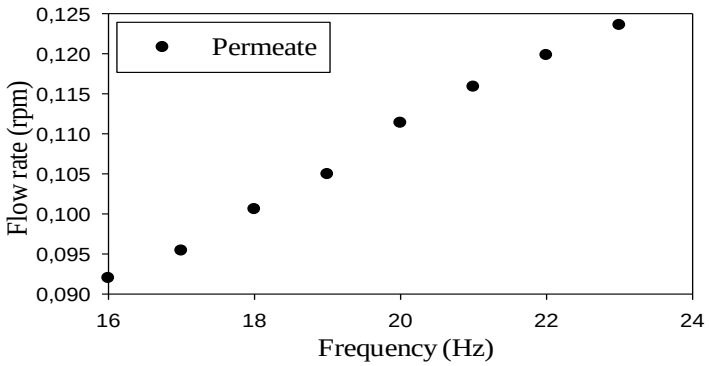

Figure 5: Variation of the permeate flow rate depending on the operating frequency of motor.

B. Filtration of synthetics solution

Figures 6, 7 and 8 present the curves obtained from the filtration of synthetic solutions of three salts at operating parameters previously determinated. The profiles of these curves are identical with remarkable difference in the operating time before reaching the plate.

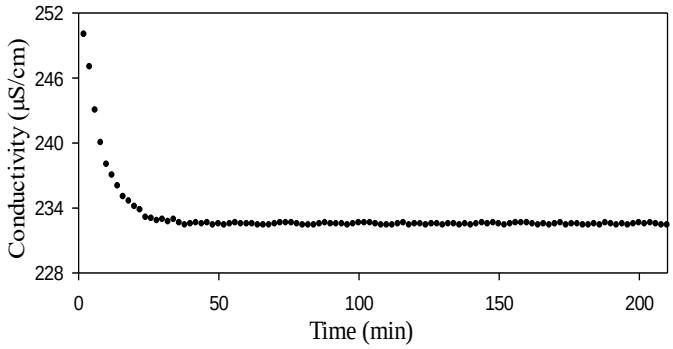

Figure 6: Permeate conductivity (sodium chloride solution)

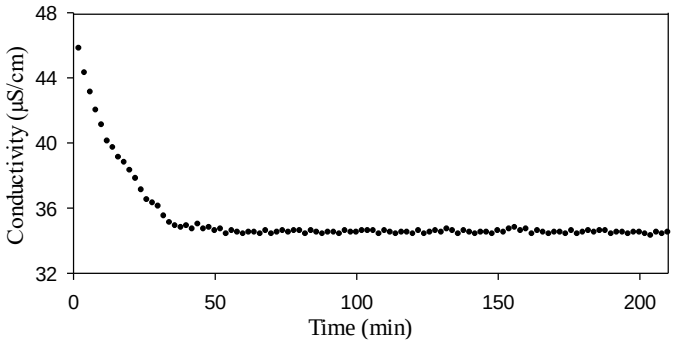

Figure 7: Permeate conductivity (sodium sulfate solution).

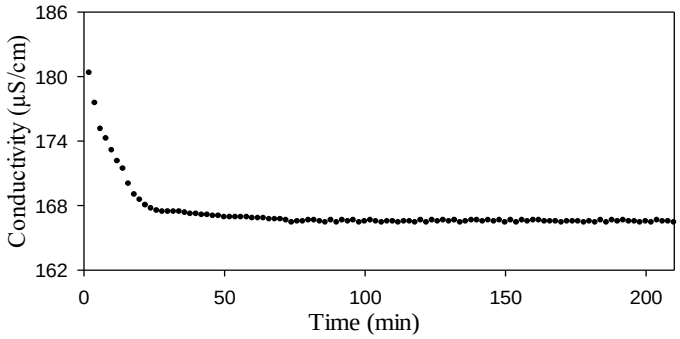

Figure 8: Permeate conductivity (sodium bicarbo-nate solution).

Table 3 summarizes for filtration of each salt solution, the retention rate, the time after which the permeate conductivity reaches a plate and the corresponding conductivity.

Table 3: Curves characteristics

Parameters	**Sodium chloride**	**Sodium sulfate**	**Sodium bicarbonate**
Time ($\boldsymbol{min}$)	24	34	22
Conductivity ($\boldsymbol{\mu S/cm}$)	233	35	167
Retention rate (%)	96	99	97

Regarding tests on the sodium chloride solution, the permeate conductivity measured at the starting of filtration is 250 µS/cm. This conductivity decreases and reaches a plate around 233 µS/cm, 24 minutes after starting of filtration. The retention rate of sodium ions and chloride ions through the membrane is estimated to 96%. For the solution of sodium sulfate, the permeate conductivity measured at the starting of filtration is 45.8 µS/cm. It decreases to reach a plate around 35 µS/cm, 38 minutes after starting of filtration. The retention rate of sulfate and sodium ions through the membrane is estimated to 99%. For the solution of sodium bicarbonate, the permeate conductivity measured at the starting of filtration is 180.3 µS/cm. It decreases until reaching a plate around 166 µS/cm, 28 minutes after starting of filtration. The retention rate of bicarbonate and sodium ions through the membrane is estimated to 97%.

Although the synthetic solutions containing salts were prepared with almost equal conductivities, the difference between conductivities of permeates resulting from the filtration of these solutions is very remarkable. The difference of these permeates conductivities is closely related to the retention rate of the membrane for each of the ions involved. The sodium chloride solution is composed exclusively of the monovalent ions Cl^- and Na^+; its retention rate is the lowest. This confirms that monovalent ions are less retained than polyvalent ions [17]. The solution of sodium bicarbonate is composed of Na^+ and HCO^{3-} ; its retention rate is lower than that of the solution of sodium sulphate so the ions involved are Na^+ and SO_4^{2-}. It is seen that the molecular structure of the SO_4^{2-} ions is denser than that of the HCO^{3-} ions. This confirms that the retention rate is also related to the molecular structure of the ions involved [18].

C. Filtration of natural water

Physicochemical properties of natural water

Table 4, presents results obtained from in-situ analyzes of Borehole C, Well R and Well L samples. For the three sampling points, the values of turbidity and pH meets WHO standards for consumer water, ie 5 NTU. For the dissolved oxygen, only the sample from Well R complies with the standard. The value of dissolved oxygen obtained can promote the growth of microorganisms that degrade organic matter [19]. The samples from Borehole C and Well L are under-oxygenates. The low values of dissolved oxygen in these two samples can promote the development of pathogens. Measured conductivities are higher than WHO standards. However, compared to other standards, such as of European Union fixed at 1000 µS/cm, the conductivity of Borehole C is acceptable. We notice considerable difference between conductivity of Borehole C compared to the two other samples that are rather closely. This discrepancy is explained by the proximity of these two sampling points with industrial sites located in Figuil. Then, these two wells are permanently in contact with ambient air saturated by particles from activities of industrial companies. The activities of these companies are based essentially on the processing of mineral materials [14]. The values of total dissolved solids are higher in the three samples. There is reason to wonder about the order of magnitude of these values, in terms of low turbidity values that are normally related to the TDS and suspended solids.

Table 4: Analyses in situ

Paramètres	Borehole C	Well R	Well L	OMS
Turbidity (NTU)	0.45	0.5	0.46	5
Conductivity ($\mu S/cm$)	688	1608	1823	400
TDS (ppm)	233	653	693	500
pH	7.31	7.49	7.25	6.5-8.5
OD (mg/l)	2.6	7	3.64	≥5
Température (°C)	29	29.9	31	/

Table 5 presents results obtained from laboratory. It appears that, the concentration of chloride is important in the three samples, compared with the standards for consumption water. This result suggests that this water are laxative and corrosive. High value of chloride resulting also from mining activities near the sampling points [19]. These mining activities spewing of mineral particles emitted firstly when crushing limestone blocks and their transport hopper to the loading area for trucks at the plant, and in the other hand, during manufacturing operations of marble tiles, cement and lime [14]. The concentrations of sulfate, phosphate, nitrate and iron are within reasonable proportions in the three samples analyzed. The concentrations of nitrite are higher in the three samples compared to WHO standards. TAC, TH, TCa and TMg are very important, compared to WHO standards. The total hardness is so high because of the lithology of the aquifer, and in particular to the significant presence of magnesium and calcium in the soils of the study area. On the other hand, limestone is considered as one of the most used materials by local industries; this can justify the high value of calcium hardness content [14]. We can note that, physicochemical analyses results show that water from the sampling points are not good for consumption.

Table 5: Laboratory analyses

Parameters	Borehole C	Well R	Well L	OMS
DCO	18	43.5	64	/
Cl^- (mg/l)	950±0.1	2870±0.02	2530±0.1	250
SO_4^{2-} (mg/l)	18.04±2.55	40.14±0.42	32.94±2.97	250
PO_4^{3-} (mg/l)	0.005±0.019	0.071±0.026	0.358±0.46	5
NH_4^+ (mg/l)	0.5	0.4	4	1.5
NO_3^-(mg/l)	3.41±0.9	17.17±0.67	18.4±0.81	50
NO_2^-(mg/l)	8	20	13	0.1
Fer (mg/l)	0	0.031±0.008	0.066±0.008	0.2
TA (M)	0.026	0.0305	0.0295	0.0027
TAC (M)	0.0475	0.0515	0.0475	0.005
TH (°F)	543±0.07	769±0.29	719±0.31	15 à 50
TCa (mg/l)	2050±0.02	2620±0.09	3050±0.1	100
TMg (mg/l)	3380±0.1	5070±0.2	4140±0.41	50

D. Results of desalination tests

Following physicochemical analyzes, reverse osmosis filtration tests were performed on water from the sampling points. Table 6 shows the results of analysis on the different permeate compared to feed water. The permeates obtained from filtration of each samples present a retention rate of 100% for sulfate, ammonium, nitrate, nitrite and iron. Residues of chloride are present in the three permeates at very low concentrations. Total hardness is reduced to acceptable proportions, because lower content may cause corrosion effect [13]. The exhaustive exploitation of this table shows that the concentrations of certain minerals in the permeates are below the levels required for consumer water. The solution to be adopted is to bid these permeates by mineral salts necessary for the human body such as calcium, magnesium, sulfate, etc ... in proportions consistent with the standards for consumer water.

Table 6 : Comparison permeate to feed water

	Borehole C		Well R		Well L	
Parameters	**Feed water**	**Permeate**	**Feed water**	**Permeate**	**Feed water**	**Permeate**
Cl^- (mg/l)	950±0.1	0.23±0.04	2870±0.02	0.11±0.00	2530±0.1	0.10±0.02
SO_4^{2-} (mg/l)	18.04±2.55	0.00	40.14±0.42	0.00	32.94±2.97	0.00
PO_4^{3-} (mg/l)	0.005±0.019	0.00	0.071±0.026	0.00	0.358±0.46	0.00
NH_4^+ (mg/l)	0.5	0.00	0.4	0.00	4.00	0.00
NO_3^-(mg/l)	3.41±0.9	0.00	17.17±0.67	0.00	18.4±0.81	0.00
NO_2^-(mg/l)	8.00	0.00	20	0.00	13.00	0.00
Fer (mg/l)	0.00	0.00	0.031±0.008	0.00	0.066±0.008	0.00
TDS	233.00	13.08	653.00	39.24	693.00	43.74
TA(M)	0.026	0.0003	0.0305	0.0003	0.0295	0.0003
TAC(M)	0.0475	0.0005	0.0515	0.0004	0.0475	0.0005
TH (°F)	543±0.07	23±0.04	769±0.29	26±0.04	719±0.31	21±0.04
TCa (mg/l)	2050±0.02	10.00	2620±0.09	30.00	3050±0.1	0.00
TMg (mg/l)	3380±0.1	0.00	5070±0.2	0.00	4140±0.41	40.00

E. Evaluation of PV power

Fig.9 is the Simulink model for sizing photovoltaic power to supply the desalination unit. On the basis of this model, it is easier to dimmer a brackish water desalination unit to obtain the PV power to be installed. Tests were carried out with parameters obtained from the filtration of the Lamorde sample. The PV power to be installed in this practical case was estimated at 335 W.

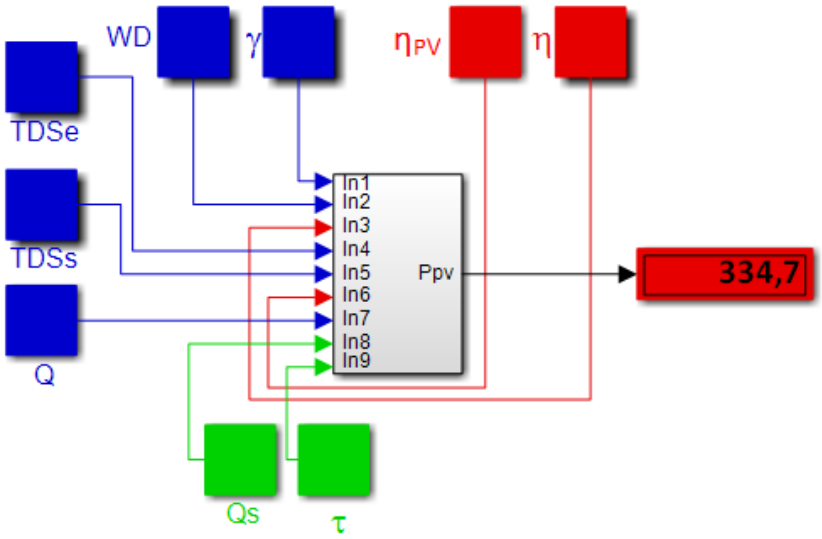

Figure 9: Simulink Model of PV power dimensioning

IV. CONCLUSION

Works contained in this paper are intended to determinate operating parameters necessary for functioning of desalination brackish water unit in remotes rural areas. Tests at different operating frequencies of the motor made it possible to determine the range of frequencies allowing the system to operate under a balanced and stable regime. Filtration tests carried out on synthetic solutions of sodium chloride, sodium sulfate and sodium bicarbonate made it possible to determine the retention rate of the membrane for each of these mineral salts. The physicochemical analysis of natural water from wells in Figuil/Cameroon shows that these water do not respect WHO standards. We note the presence of mineral pollution, consequence of high values of conductivities. These water are also tough, because of high values of calcium hardness and magnesium hardness. Filtration tests on natural water samples using operating parameters previously determined have enabled reduction the content of salts to rate recommended for consumption water. The results obtained from evaluation of parameters such as permeate flow rate, retention rate and photovoltaic power to be installed show that this desalination unit is suitable for the remotes rural areas.

Conflict of interest: The authors declare that they have no conflict of interest.

Ethical statement: The authors declare that they have followed ethical responsibilities

REFERENCES

[1] M.A. Jones, I. Odeh, M. Haddad, A.H. Mohammad and J.C. Quinn. Economic analysis of photovoltaic (PV) powered water pumping and desalination without energy storage for agriculture. Desalination 387 (2016) 35–45.

[2] Antonio Joyce, David Loureiro, Carlos Rodrigues and Susana Castrob. Small reverse osmosis units using PV systems for water purification in rural places. Desalination 137 (2001) 39-44.

[3] Eyad S. Hrayshat. Brackish water desalination by a standalone reverse osmosis desalination unit powered by photovoltaic solar energy. Renewable Energy 33 (2008) 1784–1790.

[4] Chippaux J.P., Houssier S., Gross P., Bouvier C. et Brissaud F. Etude de la pollution de l'eau souterraine de la ville de Niamey, Niger, Santé publique. Manuscrit n°2322 (2002).

[5] Ngounou Ngatcha B., Lewa S. and Ekodeck G. E. Problématique de L'Accès à L'Eau Potable Dans la Ville de Ngaoundéré (Centre Nord-Cameroun). European Journal of Scientific Research, Vol. 18, n°2, (2007), pp 223-230.

[6] Kristin Seeber, Djoret Daïra, Aminu Magaji Bala et Sara Vassolo. Études de la qualité des eaux souterraines dans la plaine d'inondation du Logone inférieur. Bundesanstalt fur Geowissenschaften und Rohstoffe, Hanovre, rapport n°7 (2014), 48 pages.

[7] Mohamed A. Eltawil, Zhao Zhengming and Liqiang Yuan. Renewable energy powered desalination systems: Technologies and economics-state of the art. Twelfth International Water Technology Conference, IWTC12 2008 Alexandria, Egypt.

[8] Benatiallah A., Mostefaou R. and Bradja K. Performance of Photovoltaic Solar System in Algeria. Desalination, Volume 209 (2007), pp 39–42.

[9] Boussaibo A., Kamta M., Kayem J., Haragus S., Muntean N. and Turi G. Analysis Mathlab/Simulink of a PV System Used for Water Pumping. Journal of Electrical and Electronics Engineering, vol. 8, n°1, (2015), pp 37-41.

[10] Venkataraman, Kartik, Joshua Ortegon, Venkatesh Uddameri and Rick Dyke. GIS Based Mapping of Wing-Powered Desalination Potential in South Texas. AWRA 2012 Spring Specialty Conference, New Orleans, LA. AWRA, 26-28 Mar. 2012. Web. 6 Dec. 2012.

[11] Eyad S. Hrayshat. Brackish water desalination by a stand alone reverse osmosis desalination unit powered by photovoltaic solar energy. Renewable Energy 33 (2008) 1784–1790.

[12] Jill Kjellsson. The Potential for Solar-Powered Desalination of Brackish Groundwater in Texas. 394K – GIS in Water Resources 2012.

[13] Rodier J. et col. L'Analyse de l'eau. Dunod, Paris, 9e edition (2009). 1579p.

[14] Oumarou Toumba et Anselme Wakponou. Exploitation minière dans l'arrondissement de Figuil (Cameroun) : Problèmes de santé publique et effets environnementaux. Belgeo [En ligne], mis en ligne le 20 décembre 2014, consulté le 28 juillet 2016. URL : http://belgeo.revues.org/14853.

[15] Ghélici N. (1993), Etude du régime transitoire de démarrage rapide d'une pompe centrifuge, Thèse de doctorat. Ecole Nationale Supérieure d'Arts et Métiers, septembre 1993.

[16] Arkhangelsky E., Kuzmenko D. and Gitis V. Impact of chemical cleaning on properties and functioning of polyethersulfone membranes, Journal of Membrane Science, Volume 305, (2007), pp 176–184.

[17] Firdaous L., Quéméneur F., Sclumpf J. P., Maleriat J. P., Jaouen P. Modification of the ionic composition of salt solutions by electrodialysis, Desalination, 2004, 167, 397.

[18] Walha K., Ben Amar R., Quemeneur F., Jaouen P.. Déminéralisation des eaux saumâtres du sud tunisien par électrodialyse ou par osmose inverse. Journal de la Société Chimique de Tunisie, 2007, 9, 133-142

[19] Belghiti M.L., Chahlaoui A. , Bengoumi D., El Moustaine R. Etude de la qualité physico -chimique et bactériologique des eaux souterraines de la nappe plio-quaternaire dans la région de Meknès (MAROC). Larhyss Journal, ISSN 1112-3680, N°14, Juin 2013, pp. 21-36.

